


RESEARCH

Open Access



The incomplete circle of Willis is associated with vulnerable intracranial plaque features and acute ischemic stroke

Huiying Wang^{1†}, Lianfang Shen^{2†}, Chenxi Zhao², Song Liu³, Gemuer Wu⁴, Huapeng Wang², Beini Wang², Jinxia Zhu⁵, Jixiang Du⁶, Zhongying Gong^{6*}, Chao Chai^{7,8*} and Shuang Xia^{7,8*} 

Abstract

Background The circle of Willis (CoW) plays a significant role in intracranial atherosclerosis (ICAS). This study investigated the relationship between different types of CoW, atherosclerosis plaque features, and acute ischemic stroke (AIS).

Methods We investigated 97 participants with AIS or transient ischemic attacks (TIA) underwent pre- and post-contrast 3T vessel wall cardiovascular magnetic resonance within 7 days of the onset of symptoms. The culprit plaque characteristics (including enhancement grade, enhancement ratio, high signal in T₁, irregularity of plaque surface, and normalized wall index), and vessel remodeling (including arterial remodeling ratio and positive remodeling) for lesions were evaluated. The anatomic structures of the anterior and the posterior sections of the CoW (A-CoW and P-CoW) were also evaluated. The plaque features were compared among them. The plaque features were also compared between AIS and TIA patients. Finally, univariate and multivariate regression analysis was performed to evaluate the independent risk factors for AIS.

Result Patients with incomplete A-CoW showed a higher plaque enhancement ratio ($P=0.002$), enhancement grade ($P=0.01$), and normalized wall index (NWI) ($P=0.018$) compared with the patients with complete A-CoW. A higher proportion of patients with incomplete symptomatic P-CoW demonstrated more culprit plaques with high T₁ signals (HT₁S) compared with those with complete P-CoW ($P=0.013$). Incomplete A-CoW was associated with a higher enhancement grade of the culprit plaques [odds ratio (OR):3.84; 95% CI: 1.36–10.88, $P=0.011$], after adjusting for clinical risk factors such as age, sex, smoking, hypertension, hyperlipemia, and diabetes mellitus. Incomplete symptomatic P-CoW was associated with a higher probability of HT₁S (OR:3.88; 95% CI: 1.12–13.47, $P=0.033$), after adjusting for clinical risk factors such as age, sex, smoking, hypertension, hyperlipemia, and diabetes mellitus. Furthermore, an irregularity of the plaque surface (OR: 6.24; 95% CI: 2.25–17.37, $P<0.001$), and incomplete symptomatic P-CoW (OR: 8.03, 95% CI: 2.43–26.55, $P=0.001$) were independently associated with AIS.

[†]Huiying Wang and Lianfang Shen contributed equally to this work

*Correspondence:
Zhongying Gong
13212121250@163.com
Chao Chai
chaichao@nankai.edu.cn
Shuang Xia
xiashuang77@163.com

Full list of author information is available at the end of the article



© The Author(s) 2023. **Open Access** This article is licensed under a Creative Commons Attribution 4.0 International License, which permits use, sharing, adaptation, distribution and reproduction in any medium or format, as long as you give appropriate credit to the original author(s) and the source, provide a link to the Creative Commons licence, and indicate if changes were made. The images or other third party material in this article are included in the article's Creative Commons licence, unless indicated otherwise in a credit line to the material. If material is not included in the article's Creative Commons licence and your intended use is not permitted by statutory regulation or exceeds the permitted use, you will need to obtain permission directly from the copyright holder. To view a copy of this licence, visit <http://creativecommons.org/licenses/by/4.0/>. The Creative Commons Public Domain Dedication waiver (<http://creativecommons.org/publicdomain/zero/1.0/>) applies to the data made available in this article, unless otherwise stated in a credit line to the data.

Conclusions This study demonstrated that incomplete A-CoW was associated with enhancement grade of the culprit plaque, and incomplete symptomatic side P-CoW was associated with the presence of HT₁S of culprit plaque. Furthermore, an irregularity of plaque surface and incomplete symptomatic side P-CoW were associated with AIS.

Keywords Circle of Willis, Intracranial atherosclerosis, Magnetic resonance imaging, Ischemic stroke, Transient ischemic attack

Background

Intracranial atherosclerosis (ICAS) is the main cause of acute ischemic stroke (AIS) and transient ischemic attacks (TIA) [1, 2]. ICAS accounts for 30–50% of the AIS cases in Asian countries [3]. Neurologic disorders, including ischemic stroke represent major public health and economic burden worldwide [4, 5]. Furthermore, greater than 50% stenosis of the major intracranial arteries are associated with AIS or TIA [6, 7]. Computed tomography angiography, cardiovascular magnetic resonance (CMR) angiography (CMRA), and rotational digital subtraction angiography (DSA) studies have shown that the stenosis of intracranial vessels is a vital imaging-based marker in individuals suspected with TIA and stroke [8]. However, the complex pathological features of atherosclerotic plaques cannot be explained by the degree of lumen stenosis alone [9, 10]. Moreover, vessel remodeling contributes to the plaque burden in addition to stenosis. High-resolution vessel wall imaging (HR-VWI) is widely used to evaluate the morphology of the intracranial atherosclerotic plaques [8]. Several studies evaluated the degree of stenosis in the affected arteries using this imaging technique [11–16]. HR-VWI studies have improved the understanding regarding the relationship between vascular pathology and the plaque features of intracranial atherosclerosis.

The circle of Willis (CoW) is an anatomical structure that connects the anterior and posterior blood circulation in the brain and is incomplete in a majority of the individuals [17–19]. Stable cerebral blood flow is maintained under normal conditions despite significant differences in the CoW among individuals [20]. The relationship between the CoW variants and acute ischemia is unclear. De Caro et al. reported a higher prevalence of CoW variants in stroke patients [21]. Furthermore, recent studies have shown that geometric variations of the intracranial vessels affected the formation and progression of ICAS [22, 23]. It was reported that atherosclerosis plaques tended to occur in arterial branches, curvatures and bifurcations because these sites were characterized by low, disturbed or oscillating blood flow [24]. There are many arterial bifurcations and tortuous parts at the downstream (bilateral middle, anterior, and posterior cerebral arteries) of the CoW. Previous study demonstrated that incomplete CoW influenced distribution

of the middle cerebral artery (MCA) plaques because of changes in the wall shear stress [25]. The variations in CoW play a decisive role in the development of atherosclerosis [20, 26]. However, the mechanisms by which variations in CoW cause downstream large vessel atherosclerosis have not been well characterized.

We hypothesized that the CoW variants were associated with different plaque characteristics and induced AIS in patients with symptomatic ICAS. Therefore, in the present study, we evaluated the association between the CoW variants and different culprit plaque features such as hyperintensity in T₁-weighted image, irregularity, positive remodeling, and enhancement grade. We also assessed if the incomplete CoW and plaque features were independent predictors of AIS.

Methods

Patient selection

This retrospective study was approved by the Ethics Committee of Tianjin First Central Hospital which waived informed consent. A total of 441 patients were identified for this study. The inclusion criteria were as follows: (1) the patients were admitted through the emergency department at our institution between September 2016 and December 2021 due to clinical symptoms of AIS or TIA, and underwent head cardiovascular magnetic resonance (CMR) examinations within 7 days of admission. TIA was defined as a transient onset of neurological dysfunction caused by focal brain ischemia without new infarction on Diffusion-weighted image (DWI) [27]; (2) the patients were 18 years of age or older; (3) stenosis (30–99%) of the large intracranial arteries were confirmed by the time of flight CMR angiography (TOF-CMRA) or strategically acquired gradient echo CMRA (STAGE-CMRA) [27, 28]; (4) with no intravascular intervention before the high-resolution CMR vessel wall examination; (5) detection of atherosclerotic plaques by HR-VWI in at least one of the major intracranial arteries considered as the etiology of the ischemic events; (6) good imaging quality to evaluate plaques and stenosis; (7) the symptomatic side of TIA patients can be confirmed.

The exclusion criteria were as follows: (1) patients with a history of non-atherosclerotic cerebrovascular diseases

such as arthritis, Moyamoya disease, aneurysm, or dissection; (2) co-existence of more than 30% stenosis in the internal carotid artery, basilar artery, vertebral artery, or common carotid artery upstream of the CoW; (3) evidence of cardioembolic and aortic arch atherosclerosis; (4) contraindications to CMR or gadolinium contrast agents. National Institute of Health Stroke Scale (NIHSS) scores of the patients were evaluated by a neurological physician (J.X.D. with 5 years of experience and blinded to the imaging information) on the day of the HR-VWI examination. To determine the symptomatic side, two neurological physicians (J.X.D. and Z.Y.G. with 5 and 20 years of experience, respectively) based on the neurodiagnostic tests and detailed histories to identify brain injury and its vascular genesis according to the statement of American Heart Association/American Stroke Association Stroke Council [27, 29]. They were both blinded to the imaging information. The major risk factors for ICAS, namely, hypertension, hyperlipidemia, diabetes mellitus, and history of smoking, were also recorded for all the study subjects.

Imaging protocols

CMR was performed on a 3T scanner (MAGNETOM Prisma, Siemens Healthineers, Erlangen, Germany) equipped with the 64-channel head and neck coil. The patients were provided with head cushions and earplugs to stabilize their head and minimize motion artifacts. The patients underwent routine head CMR, CMRA, and STAGE CMRA for the intracranial arteries. Firstly, DWI acquisitions were performed to locate the AIS lesions. Then, CMRA and STAGE CMRA were used to confirm the stenosis sites in the intracranial vessels and determine the integrity of CoW as described in a previous study [30]. The stroke mechanisms were categorized and analyzed according to DWI and CMRA (presented in the Additional file 1). Sagittal pre-contrast HR-VWI was performed using the Inversion-recovery prepared sampling perfection with application-optimized contrast using different flip angle evolutions (IR-SPACE) to evaluate the characteristics of all intracranial plaques [31]. Dynamic susceptibility contrast-enhanced perfusion weighted imaging (DSC-PWI) was used to detection of perfusion abnormalities, especially for TIA patients [32]. It was performed by injecting the gadolinium-based contrast agent (Magnevist; Schering, Berlin, Germany) at a dose of 0.2 ml/kg at a rate of 4 mL/s. Then, post-contrast IR-SPACE was performed to evaluate the enhancement characteristics of all intracranial plaques. The imaging sequence parameters are listed in Additional file 1: Table S1.

Image analysis

Plaque identification on HR-VWI

All the CMR images were analyzed independently by 2 neuroradiologists (H.Y.W. and C.X.Z. with 7- and 5-years' experience, respectively), who were blinded to the clinical information of the patients. The symptomatic sides of TIA patients were confirmed through the neurodiagnostic tests, detailed clinical histories, and CMR imaging (vessel stenosis from CMRA, perfusion abnormalities from DSC-PWI) according to previous studies [27, 32] (a case presented in Additional file 1: Fig. S1). The HR-VWI source and multiplanar reformation (MPR) images displayed on the RadiAnt DICOM Viewer2021.1 workstation are shown in Additional file 1: Fig. S2. The observers carefully inspected the large intracranial arteries, including anterior cerebral arteries (up to the A2 segment), middle cerebral arteries (up to the M2 segment), and posterior cerebral arteries (up to the P2 segment) for the presence of plaques. When the thickness of the vessel wall was greater than 50% of the adjacent normal vessel wall in both the pre- and post-contrast IR-SPACE images [33, 34], the distinct area was defined as a plaque shown in Fig. 1. The reference vessel wall was defined as the adjacent proximal, distal, or contralateral cross-section with a thin, smooth vessel wall (Fig. 1). The plaques were designated as culprit plaques based on the following criteria: (1) the only atherosclerotic lesion within the vascular territory of the stroke or TIA; or (2) the lesion with maximum stenosis when multiple plaques were present within the same responsible artery [15] (Additional file 1: Fig. S3). A plaque was considered as a non-culprit plaque when it was not within the vascular territory of the ischemic events. Plaques were categorized as culprit or non-culprit plaques by 2 independent neuroradiologists (G.M.W. and S.L. both with 7- years' experience), who were provided with the clinical information, routine CMR images, and TOF-CMRA (or STAGE-CMRA) for the analysis. To avoid potential bias, they were not provided with HR-VW images. Quantitative and qualitative measurements of the individual plaques were performed using cross-sectional views of the HR-VWI images by two independent observers (H.Y.W. and C.X.Z. with 7- and 5-years' experience, respectively). In case of any discrepancies between the two observers, the presence of a plaque was determined by a third senior observer (S.X. with 20-years' experience in neuroradiology). After four weeks, one of the neuroradiologists (H.Y.W. with 7- years of experience) measured the quantitative and qualitative data for a cohort of 30 randomly chosen patients.

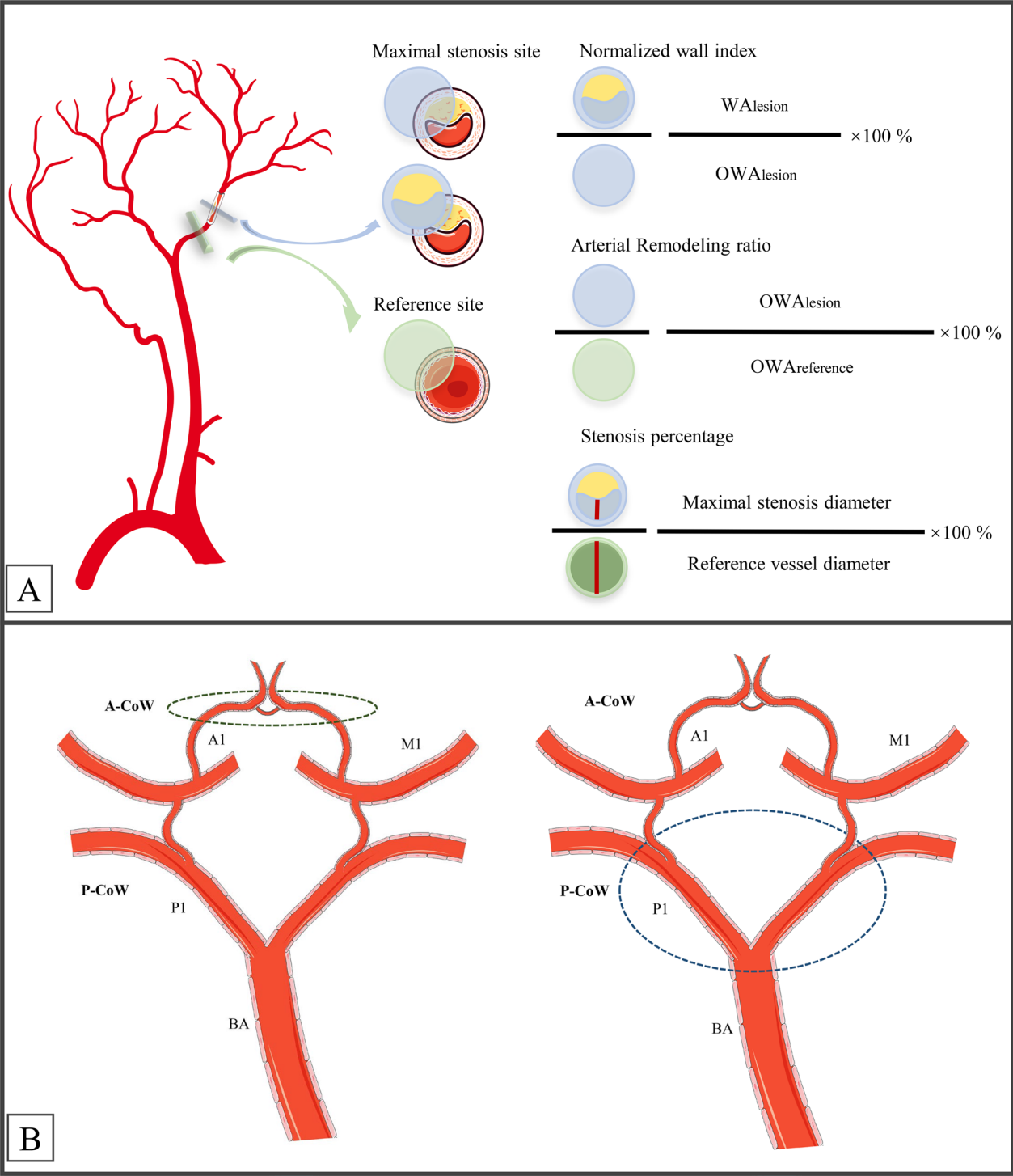


Fig. 1 The schematic diagram of the circle of Willis (CoW) and the measurement formulas of lesions. **A** Methodology used to measure the normalized wall index, arterial remodeling ratio, and stenosis percentage. **B** Evaluation of the CoW. The CoW was divided into anterior- and posterior-CoW (A-CoW and P-CoW, respectively) sections. A-CoW consists of bilateral A1 segments and the anterior communicating artery. P-CoW consists of the bilateral P1 segments and the bilateral posterior communicating arteries. P-CoW was further categorized into incomplete and complete symptomatic sides

Evaluation of plaque burden and measurement of plaque features

The minimal lumen diameter at the site of maximal stenosis was measured for each stenosis vessel segment and divided by the diameter of the reference vessel wall to yield the stenosis percentage [15] (Fig. 1). The wall area of the lesion (WA_{lesion}), the outer wall area of the lesion (OWA_{lesion}), and the lumen area of the reference ($LA_{\text{reference}}$) were measured using the formulas listed in Fig. 1. The normalized wall index (NWI) was calculated as $WA_{\text{lesion}} / OWA_{\text{lesion}} \times 100\%$ [35]. The arterial remodeling ratio (ARR) was calculated as $(OWA_{\text{lesion}} / OWA_{\text{reference}}) \times 100\%$ (Fig. 1). $ARR > 1.05$ was considered

as positive remodeling, whereas $ARR < 0.95$ was considered as negative remodeling [36].

The mean signal intensity (SI) was measured within the regions-of-interest (ROIs), which were manually drawn in the brightest region of each identified plaque (SI_{plaque}), the reference vessel wall (SI_{ref}), and the pituitary infundibulum (SI_{infund}) (Additional file 1: Fig. S4). The plaque signal in T_1 weighted image was considered when the signal intensity was greater than 150% ($SI > 150\%$) relative to the signal of the reference wall in the pre-contrast IR-SPACE [15]. The contrast enhancement ratio (CER) was quantified with the slice of greatest enhancement using the contralateral side of the brain parenchyma to

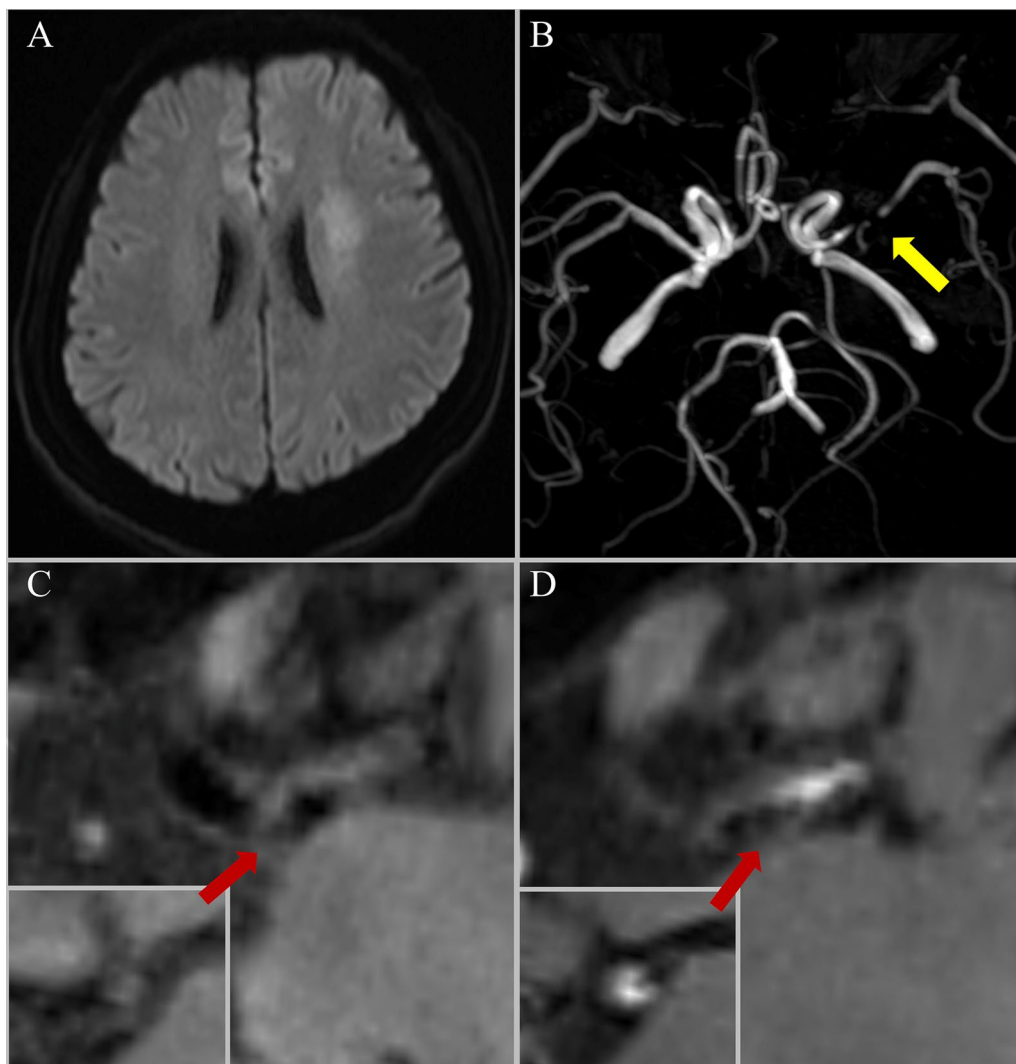


Fig. 2 Representative case of a 58-year-old woman who was diagnosed with stroke before performing the CMR scan. **A** Diffusion weighted imaging (DWI) showed high signal intensity lesions on the left centrum ovale. **B** time of flight cardiovascular magnetic resonance angiography (TOF-CMRA) showed severe stenosis (yellow arrow) in the left middle cerebral artery (MCA) M1. **C, D** Curved multiplanar reconstructions of the **C** pre-contrast and **D** post-contrast HR-VWI showed a focal plaque in the left MCA with severe stenosis (stenosis ratio = 87.25%), irregular plaque surface, and grade 2 enhancement (plaque enhancement ratio = 3.13)

normalize the signal intensity. The contrast enhancement ratio was estimated with the following formula: $[(\text{signal of plaque}_{\text{post-contrast}}/\text{signal of contralateral brain parenchyma}_{\text{post-contrast}})/(\text{signal of plaque}_{\text{pre-contrast}}/\text{signal of contralateral brain parenchyma}_{\text{pre-contrast}})] \times 100\%$ [37]. The lesion enhancement was classified into the following grades based on the post-contrast IR-SPACE: grade 0, $SI_{\text{plaque}} \leq SI_{\text{ref}}$; grade 1, $SI_{\text{ref}} < SI_{\text{plaque}} < SI_{\text{infund}}$; grade 2, $SI_{\text{plaque}} \geq SI_{\text{infund}}$. We also recorded the plaque surface irregularity (defined as discontinuity of the plaque inner surface; Fig. 2) and regularity (smooth inner surface; Additional file 1: Fig. S5).

Analysis of the circle of Willis

The axial STAGE-CMRA source images containing 64 slices were obtained by post-processing the STAGE images using the STAGE software 1.2.1 (SpinTech, Bingham Farms, Michigan, USA) [28]. The structural characteristics of the CoW were evaluated using STAGE-CMRA or TOF-CMRA if either was available and STAGE-MRA if both were available. The type of CoW was analyzed by the two neuroradiologists (G.M.W. and S.L. with 7- years' experience) using the original images as well as MIP images according to previously published criteria [30]. The anatomical structures of the CoW were divided into the anterior and posterior sections (Fig. 1) to determine the following types: (1) for the anterior CoW (A-CoW) section, type I with complete and normal anterior circulation vessels; type II with incomplete or dysplasia in the anterior half; (2) for the posterior CoW (P-CoW) section, type III with complete and normal in the symptomatic side of the posterior half (defined as normal and complete components of the P-CoW in the symptomatic side of the patients with clinical symptoms); type IV, incomplete or dysplasia in the symptomatic side of the posterior half (Fig. 1).

Statistical analysis

The statistical data analysis was performed using the SPSS (version 22.0, Statistical Package for the Social Sciences, International Business Machines, Inc., Armonk, New York, USA) and GraphPad Prism (version 8.3.0, GraphPad Software, San Diego, California, USA) software. The quantitative data are presented as means \pm standard deviation (SD) for normally distributed data or median (interquartile range, IQR) for data with skewed distributions. Categorical variables were expressed as counts (percentages). The intraclass correlation coefficient (ICC) (for continuous variables)/ Weighted kappa (for categorical variables)/ Cohen's kappa (for binary variables) were conducted to measure inter-rater reliability and intra-reader reproducibility. The statistical differences in the

culprit plaque features and the clinical data between patient groups with different types of CoW were determined using the two independent sample t-test for normally distributed quantitative data, the Mann-Whitney U-test for skewed distributions data, and the chi-square test or Fisher's exact test for categorical data. Univariate binary logistic analysis was used to evaluate the association between different types of CoW and plaque characteristics such as the presence of high T_1 signal (HT_1S), irregularity of plaque surface, and positive remodeling. Univariate ordinal regression analysis was performed to determine the association between the types of CoW and culprit plaque enhancement grade. The variables with P -value < 0.1 were included in the multivariate regression analysis, which was conducted by adjusting for age, sex, and clinical risk factors, including a history of smoking, hyperlipemia, hypertension, and diabetes mellitus.

The differences in the culprit plaque characteristics between the AIS and TIA groups were compared using the two independent sample t-test for normally distributed quantitative data, Mann-Whitney U-test for skewed distributions data, and chi-square test or Fisher's exact test for the categorical data. Univariate logistic analysis was performed to identify the variables associated with AIS, and those with P -value < 0.1 were included in multivariate analysis. Multivariate regression analysis was performed by adjusting for age, sex, and clinical risk factors, including a history of smoking, hyperlipemia, hypertension, and diabetes mellitus. Because patients with ischemic incidents may be identified with more than one plaque. The relationships between plaque characteristics and AIS were assessed using univariate and multivariate generalized estimating equations for patients with multiple intracranial plaques. A two-sided $P < 0.05$ was considered statistically significant. The receiver operating characteristic curves were performed to analyze the independent significance parameters.

Results

Demographics and basic characteristics of the study subjects

This study included 97 patients, including (62 males, age 54.1 ± 14.0 years; age range: 23–80 years old). The A-CoW was incomplete in 26 (26.8%) of the 97 AIS or TIA patients, whereas the symptomatic side P-CoW was incomplete in 72 (74.2%) of 97 (Fig. 3). DWI hyperintensity was observed in 56 patients after symptoms onset, whereas the remaining 41 patients did not show acute lesions on the DWI. In the 97 patients, 164 intracranial plaques were identified, including 97 culprit plaques and 67 non-culprit plaques (Fig. 3). The degree of stenosis caused by the culprit plaque in our study ranged from 43 to 96%. The status of the clinical risk factors

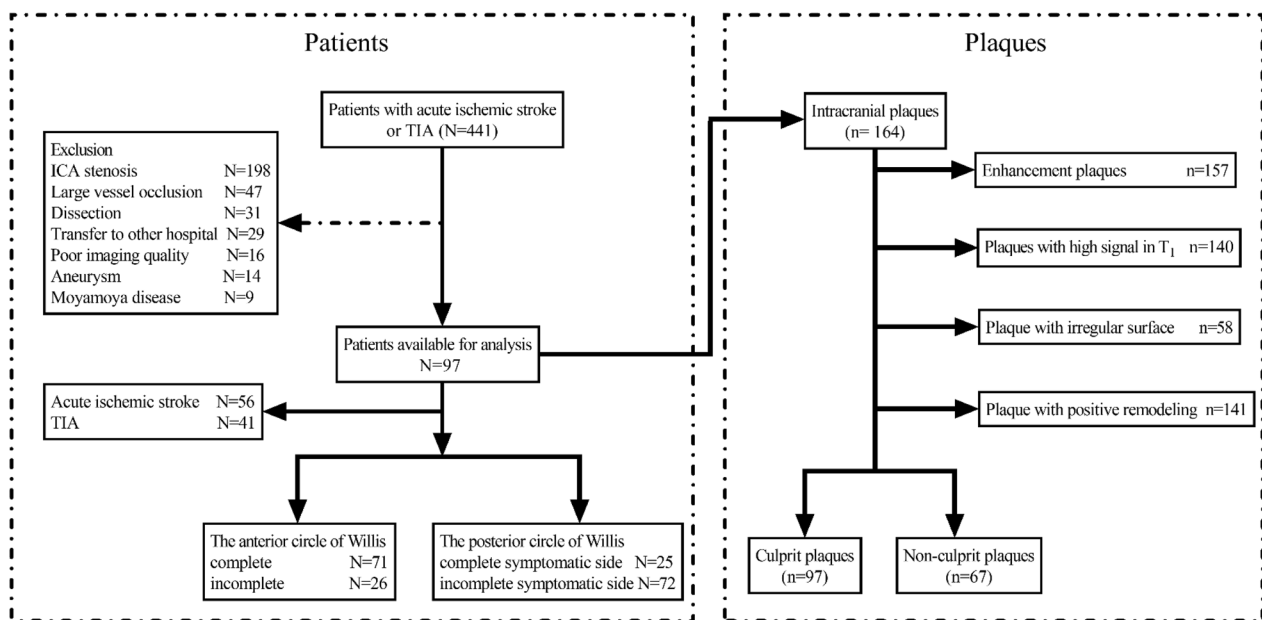


Fig. 3 Flowchart of the study subjects and classification of the vessel lesions

and the NIHSS scores of the study patients are shown in Table 1. We did not observe any significant differences in age, sex, and clinical risk factors between the AIS and TIA patients (all $P > 0.05$). However, patients with AIS [2(1, 3.75)] showed higher NIHSS scores than the patients with TIA [0(0, 2)] ($P < 0.001$; Table 1). Furthermore, this study showed significantly high inter-rater and intra-reader reliability for the plaque characteristics and arterial remodeling ratio (0.73–0.99) (Additional file 1: Table S2).

Culprit plaque features and the type of CoW among AIS and TIA groups

The culprit plaques were more frequently observed in patients with AIS and showed higher enhancement grades ($P = 0.01$) and CER ($P = 0.048$) compared with the patients with TIA (Table 1). Furthermore, irregularity of the culprit plaque surface was more commonly detected in the patients with AIS compared with the patients with TIA ($P < 0.001$) (Table 1). The presence of HT₁S in the culprit plaques of AIS patients was slightly higher than that of TIA patients ($P = 0.073$). However, we did not observe any significant differences in the arterial remodeling ratio ($P = 0.189$), stenosis percentage ($P = 0.476$), NWI ($P = 0.977$), and positive remodeling ($P = 0.102$) between the two groups. A higher percentage of AIS patients showed incomplete symptomatic side P-CoW compared with the TIA patients ($P < 0.001$). (Table 1).

Distinct characteristics of culprit plaque features in patients with incomplete anterior or posterior CoW

The culprit plaques in the patients with incomplete A-CoW showed a higher CER ($P = 0.002$), enhancement grade ($P = 0.01$), and NWI ($P = 0.018$) compared with the patients with complete A-CoW (Table 2). However, culprit plaque features such as stenosis percentage ($P = 0.538$), HT₁S ($P = 0.730$), irregularity of plaque ($P = 0.925$), arterial remodeling ratio ($P = 0.890$), and positive remodeling ($P = 0.345$) were statistically similar between the patients with complete and incomplete A-CoW (Table 2; Fig. 4). The culprit plaques in the patients with incomplete symptomatic side P-CoW showed a higher probability of HT₁S compared with the patients with complete symptomatic side P-CoW ($P = 0.013$; Table 2). The culprit plaque features such as stenosis percentage ($P = 0.247$), CER ($P = 0.610$), enhancement grade ($P = 0.931$), irregularity of plaque surface ($P = 0.760$), NWI ($P = 0.895$), arterial remodeling ratio ($P = 0.501$), and positive remodeling ($P = 0.987$) did not show any significant differences between the patients with complete and incomplete P-CoW (Table 2; Fig. 4).

Incomplete CoW types associated with specific plaque features

Incomplete A-CoW was independently associated with enhancement grade of the culprit plaques before (OR:3.40; 95% CI: 1.32–8.76; $P = 0.011$) and after adjusting for clinical risk factors such as age,

Table 1 Demographics characteristics and culprit plaque feature between AIS and TIA patients

| Characteristics | AIS (N = 56) | TIA (N = 41) | P |
|--------------------------------|--------------|--------------|---------------------------|
| Age (years old) | 53.1 ± 13.4 | 55.5 ± 14.9 | 0.418 |
| Sex (Female/Male) | 20/36 | 15/26 | 0.930 |
| Clinical history [N (%)] | | | |
| Hypertension | 39 (69.6%) | 34 (82.9%) | 0.134 |
| Hyperlipidemia | 26 (46.4%) | 22 (53.7%) | 0.482 |
| Diabetes Mellitus | 22 (39.3%) | 17 (41.5%) | 0.829 |
| Ischemic heart disease | 8 (14.3%) | 5 (12.2%) | 0.765 |
| History of stroke | 17 (30.4%) | 18 (43.9%) | 0.17 |
| Smoking | 28 (50%) | 20 (48.8%) | 0.906 |
| NIHSS scores [median (IQR)] | 2(1, 3.75) | 0(0, 2) | <0.001* |
| CoW integrity [N (%)] | | | |
| Incomplete A-CoW | 16 (28.6%) | 10 (24.4%) | 0.648 |
| Incomplete S-P-CoW | 49 (87.5%) | 23 (56.1%) | <0.001 [#] |
| Plaque features | | | |
| Stenosis percentage | 69.3 ± 13.2 | 67.3 ± 14.0 | 0.476 |
| Plaque enhancement ratio | 202.6 ± 55.2 | 179.2 ± 59.7 | 0.048 [^] |
| Enhancement grade (0/1/2) | 0/36/20 | 4/30/7 | 0.010 [#] |
| Irregularity of plaque [N (%)] | 34 (62.5%) | 10 (24.4%) | <0.001 [#] |
| NWI | 84.9 ± 11.1 | 83.9 ± 13.3 | 0.977 |
| Positive remodeling [N (%)] | 12 (21.4%) | 4 (9.8%) | 0.102 |
| Arterial remodeling ratio | 0.87 ± 0.29 | 0.79 ± 0.22 | 0.189 |
| HT ₁ S [N (%)] | 51 (91.1%) | 32 (78.0%) | 0.073 |

AIS acute ischemic stroke, TIA transient ischemic attack, A-CoW anterior circle of Willis, S-P-CoW symptomatic side posterior circle of Willis, NWI normalized wall index, HT₁S high T₁ signal

sex, smoking, hypertension, hyperlipemia, and diabetes mellitus (OR:3.84; 95% CI: 1.36–10.88; $P=0.011$) (Table 3). Incomplete symptomatic side P-CoW was associated with the presence of culprit plaque HT₁S before (OR:3.61; 95% CI: 1.12–11.61; $P=0.032$) and

after adjusting for clinical risk factors such as age, sex, smoking, hypertension, hyperlipemia, and diabetes mellitus (OR: 3.88; 95% CI: 1.12–13.47; $P=0.033$) (Table 3).

Association between culprit plaque features, types of CoW, and AIS

The univariate logistic regression analysis showed that the culprit plaque features such as irregularity of plaque surface (OR: 4.79, 95% CI: 1.96–11.69, $P=0.001$), enhancement ratio (OR: 1.01, 95% CI: 1.00–1.02, $P=0.052$), enhancement grade 2 (OR: 2.38, 95% CI: 0.89–6.39, $P=0.085$), and incomplete symptomatic side P-CoW (OR: 5.90, 95% CI: 2.07–16.87, $P=0.001$) were associated with AIS. The irregularity of culprit plaque surface (OR: 6.24, 95% CI: 2.25–17.37, $P<0.001$) and incomplete symptomatic side P-CoW (OR: 8.03, 95% CI: 2.43–26.55, $P=0.001$) were independently associated with AIS after adjustment for age, sex, and clinical risk factors such as smoking, hypertension, hyperlipemia, and diabetes mellitus (Table 4). ROC curve analysis showed that the area under the ROC curve (AUC) value was 0.682 (95% CI, 0.574–0.790) for irregularity of the plaque surface, 0.654 (95% CI, 0.540–0.768) for incomplete P-CoW, and 0.774 (95% CI, 0.681–0.867) for a combination of these two factors with a sensitivity of 90.2% and a specificity of 53.6%.

Association between features of all plaques, types of CoW, and AIS

Irregularity of plaque surfaces (OR: 1.08, 95% CI: 1.03–1.13, $P=0.002$), arterial remodeling ratio (OR: 1.06, 95% CI: 1.00–1.13, $P=0.043$), enhancement ratio (OR: 1.00, 95% CI: 1.00–1.00, $P=0.070$), enhancement grade 2 (OR: 1.23, 95% CI: 1.00–1.53, $P=0.064$), positive remodeling (OR: 1.04, 95% CI: 1.01–1.07, $P=0.024$), and incomplete

Table 2 Comparison of culprit plaque features between different types of CoW

| Culprit plaque features | Complete A-CoW | Incomplete A-CoW | P | Complete symptomatic side P-CoW | Incomplete symptomatic side P-CoW | P |
|--------------------------------|----------------|------------------|---------------------------|---------------------------------|-----------------------------------|-------------------------------|
| Stenosis percentage | 67.9 ± 13.9 | 68.8 ± 12.4 | 0.538 | 71.1 ± 14.2 | 67.5 ± 13.2 | 0.247 |
| Plaque CER | 181.8 ± 53.6 | 222.5 ± 60.1 | 0.002 [#] | 193.7 ± 50.9 | 192.4 ± 60.6 | 0.610 |
| Enhancement grade (0/1/2) | 4/52/15 | 0/14/12 | 0.010 * | 0/19/6 | 4/47/21 | 0.931 |
| HT ₁ S [N (%)] | 62(87.3%) | 21(80.8%) | 0.730 | 18(72.0%) | 65(91.6%) | 0.013 ^{&} |
| Irregularity of plaque [N (%)] | 32(45.1%) | 12(46.12%) | 0.925 | 12(48.0%) | 32(44.5%) | 0.760 |
| NWI | 83.0 ± 12.5 | 88.5 ± 9.8 | 0.018 [#] | 83.5 ± 14.3 | 84.8 ± 11.3 | 0.895 |
| ARR | 0.84 ± 0.26 | 0.82 ± 0.25 | 0.890 | 0.82 ± 0.29 | 0.84 ± 0.25 | 0.501 |
| Positive remodeling [N (%)] | 14(19.7%) | 2(7.7%) | 0.345 | 4(16.0%) | 12(16.7%) | 0.987 |

A-CoW anterior circle of Willis, P-CoW posterior circle of Willis, ER contrast enhancement ratio, HT₁S high T₁ signal; [#]Independent samples t-test, *Fisher's exact test, [&]chi-square test

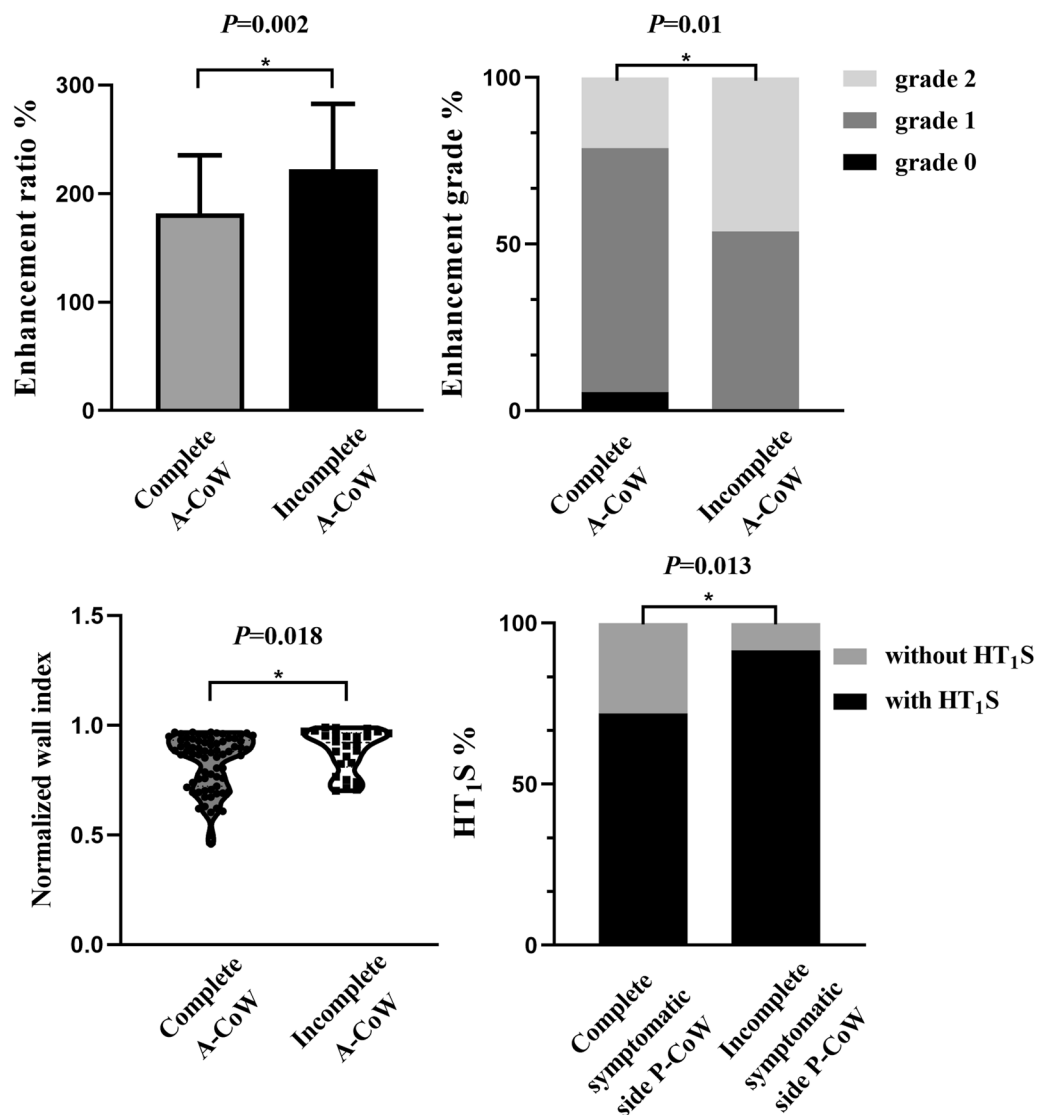


Fig. 4 Comparison of the plaque characteristics between patients with different types of CoW. (Top) In the A-CoW group, patients with incomplete A-CoW showed a higher enhancement ratio ($P=0.002$), and enhancement grade ($P=0.01$) compared with the patients with complete A-CoW. (Bottom left) Patients with incomplete A-CoW also showed a higher normalized wall index (NWI) compared with those with complete A-CoW ($P=0.018$). (Bottom right) In the P-CoW group, patients with incomplete symptomatic side P-CoW showed a higher probability of high T_1 signal (HT₁S) compared with those with complete symptomatic side P-CoW ($P=0.013$)

symptomatic side P-CoW (OR: 5.92, 95% CI: 2.07–16.92, $P=0.001$) were associated with AIS for all the intracranial plaques. Irregularity of plaque surfaces (OR: 1.01, 95% CI: 1.00–1.02, $P<0.001$), enhancement grade 2 (OR: 1.03, 95% CI: 1.00–1.07, $P=0.048$), and incomplete symptomatic side P-CoW (OR: 5.93, 95% CI: 2.08–16.94, $P=0.001$) were associated with AIS after adjustment for age, sex, and clinical risk factors such as smoking, hypertension, hyperlipemia, and diabetes mellitus (Table 5).

Discussion

Our study showed that the culprit plaque features varied significantly between patients with different types of CoW. Patients with incomplete A-CoW showed a higher CER, enhancement grade, and NWI for the culprit plaque features, whereas patients with incomplete symptomatic side P-CoW showed a higher probability of HT₁S. Moreover, incomplete A-CoW was independently associated with higher enhancement grades of the culprit plaques, whereas incomplete symptomatic side P-CoW was independently associated with a

Table 3 Association between incomplete CoW and culprit plaque features

| Incomplete CoW | Univariate regression | | | Multivariate regression | | |
|------------------------------------|-----------------------|------------|--------------|-------------------------|------------|--------------|
| | OR | 95% CI | P | OR | 95% CI | P |
| HT ₁ S | | | | | | |
| A-CoW | 1.64 | 0.49–5.45 | 0.419 | 1.555 | 0.40–6.00 | 0.522 |
| Symptomatic side P-CoW | 3.61 | 1.12–11.64 | 0.032 | 3.878 | 1.12–13.47 | 0.033 |
| Enhancement grade | | | | | | |
| A-CoW | 3.40 | 1.32–8.76 | 0.011 | 3.840 | 1.36–10.88 | 0.011 |
| Symptomatic side P-CoW | 0.28 | 1.11–6.96 | 0.924 | 0.873 | 1.54–4.94 | 0.991 |
| Positive remodeling | | | | | | |
| A-CoW | 0.29 | 0.04–2.17 | 0.226 | 0.134 | 0.01–1.34 | 0.087 |
| Symptomatic side P-CoW | 0.86 | 0.12–5.94 | 0.876 | 1.168 | 0.15–9.11 | 0.882 |
| Irregularity of the plaque surface | | | | | | |
| A-CoW | 1.05 | 0.42–2.57 | 0.924 | 1.045 | 0.40–2.75 | 0.929 |
| Symptomatic side P-CoW | 1.15 | 0.46–2.87 | 0.758 | 1.215 | 0.48–3.09 | 0.682 |

OR odds ratio, CI confidence interval, A-CoW anterior circle of Willis, P-CoW posterior circle of Willis, HT₁S high T₁ signal

Table 4 Association between vascular risk factors and acute ischemic stroke

| Culprit plaque features | Univariate regression | | | Multivariate regression | | |
|---------------------------------|-----------------------|---------------------|--------------|-------------------------|---------------------|------------------|
| | OR | 95% CI | P | OR | 95% CI | P |
| Irregularity of plaques surface | 4.791 | 1.963–11.690 | 0.001 | 6.244 | 2.245–17.368 | <0.001 |
| Enhancement ratio (%) | 1.007 | 1.000–1.015 | 0.052 | | | |
| Enhancement grade 1 | 1.003 | 0.156–1.128 | 0.927 | | | |
| Enhancement grade 2 | 2.381 | 0.887–6.393 | 0.085 | | | |
| HT ₁ S | 0.349 | 0.107–1.134 | 0.129 | | | |
| ARR (%) | 0.292 | 0.056–1.516 | 0.143 | | | |
| Incomplete S-P-CoW | 5.903 | 2.065–16.873 | 0.001 | 8.033 | 2.430–26.550 | 0.001 |

S-P-CoW symptomatic side posterior circle of Willis, HT₁S high T₁ signal, ARR arterial remodeling ratio, OR odds ratio, CI confidence interval

Table 5 Association between vascular risk factors and acute ischemic stroke

| Plaque features | Univariate regression | | | Multivariate regression | | |
|---------------------------------------------------------|-----------------------|---------------------|--------------|-------------------------|---------------------|------------------|
| | OR | 95% CI | P | OR | 95% CI | P |
| Enhancement grade (grade 1) | 1.127 | 0.932–1.363 | 0.218 | | | |
| Enhancement grade (grade 2) | 1.229 | 0.998–1.529 | 0.064 | 1.033 | 1.000–1.067 | 0.048 |
| HT ₁ S (with high signal in T ₁) | 1.041 | 0.983–1.103 | 0.168 | | | |
| Irregularity of plaque surface (with irregularity) | 1.077 | 1.028–1.128 | 0.002 | 1.010 | 1.004–1.015 | <0.001 |
| Enhancement ratio (%) | 1.001 | 1.000–1.001 | 0.070 | | | |
| Positive remodeling (with) | 1.038 | 1.005–1.073 | 0.024 | | | |
| ARR (%) | 1.064 | 1.002–1.129 | 0.043 | | | |
| Incomplete A-CoW | 1.806 | 0.322–2.021 | 0.646 | | | |
| Incomplete symptom side P-CoW | 5.920 | 2.071–16.922 | 0.001 | 5.933 | 2.079–16.935 | 0.001 |

OR odds ratio, CI confidence interval, HT₁S high T₁ signal, P-CoW posterior circle of Willis, ARR arterial remodeling ratio, A-CoW anterior circle of Willis, P-CoW posterior circle of Willis

higher probability of HT₁S in the culprit plaques. Our study also demonstrated that incomplete symptomatic side P-CoW was more commonly detected in the AIS patients compared with the patients with TIA. Furthermore, our study also showed that culprit plaques with irregularity of the plaque surface, and incomplete symptomatic side P-CoW were associated with AIS. In patients with more than one intracranial plaque, the analysis was performed by including non-culprit plaques. In such cases, the results showed that all intracranial plaques with irregularity of plaque surface, enhancement grade 2, and incomplete symptomatic side P-CoW were associated with AIS.

The collateral cerebral blood flow is mainly dependent on the CoW, especially under ischemic conditions that require compensatory changes in the blood flow [38]. However, anatomical variations have been reported in the CoW among normal individuals [39]. These anatomical variations in the CoW may be genetically predetermined and persist in all individuals since birth. The variations of CoW can alter the hemodynamics in the cerebral arteries [39, 40] and affect the wall shear stress (WSS) in the downstream artery wall [39, 41]. WSS is a widely used hemodynamic index in the study of atherosclerosis [42–44]. High WSS is associated with plaque rupture because of endothelial dysfunction and weakened plaque surface [45]. Endothelial dysfunction, neovascularization, and inflammation promote plaque enhancement because of gadolinium leakage [46]. Our study also showed that incomplete A-CoW was associated with the enhancement grade of the culprit plaques. Furthermore, our study showed that incomplete symptomatic side P-CoW was associated with HT₁S of the culprit plaques. HT₁S is related to intraplaque hemorrhage, which is associated with carotid plaque progression [47]. The size of intraplaque hemorrhage in the carotid artery is an independent predictor of stroke risk [48]. Although it lacked pathological proof between intraplaque hemorrhage and intracranial atherosclerotic plaques. Several studies have shown that intraplaque hemorrhage is a characteristic feature of the vulnerable intracranial atherosclerotic plaques and is associated with stroke [13, 49]. However, thrombosis can also show HT₁S in some studies [50], which was consistent with the signal of hemorrhage. Therefore, we thought the HT₁S in the plaque might be the hemorrhage or thrombosis or the mixture of these two components because the thrombosis can occur secondary to the hemorrhage of plaque. However, no matter the occurrence of hemorrhage or thrombosis or this mixture, it indicated that the rupture of plaque, which was always the risk factor for the stroke.

Incomplete CoW increases the risk of AIS and TIA in patients with ICAS because cerebral perfusion cannot

be maintained [21, 51]. In our study, incomplete symptomatic side P-CoW was observed in 74.2% (72/97) of the study participants and was consistent with a previous report in the study of Chinese population [30]. Our study also showed that incomplete symptomatic side P-CoW was independently associated with AIS. This suggested that the posterior communicating arteries were the primary source of collateral circulation between the anterior and posterior circulation of the brain. The posterior communicating arteries are also the origin of many penetrating arteries. If patients with P-CoW variations underwent large artery stenosis or occlusion, the brain tissue was prone to be hypoxic because they lacked sufficient compensation of collateral blood flow. Chuang et al. also reported that incomplete P-CoW was a risk factor for AIS [52]. In addition, poor integrity of CoW may relate to increased recurrent stroke in patients with severe intracranial atherosclerotic stenosis [53], and also to the poor prognosis of patients with AIS [54]. For the high-risk population with incomplete P-CoW, the progress of intracranial atherosclerosis should be closely monitored to prevent ischemic stroke. For the high-risk population with incomplete P-CoW, the progress of intracranial atherosclerosis should be closely monitored to prevent ischemic stroke. The above research confirmed that intracranial atherosclerosis patients with incomplete P-CoW may benefit from early clinical intervention (including medical treatment and intravascular treatment), post-stroke treatment and management.

In our study, the culprit plaques had a higher CER and higher enhancement grade in AIS patients than those in TIA patients. The enhancement behavior of the plaque was caused by neovascularization which reflected plaque inflammation [55]. Neovascularity was associated with the accumulation of inflammatory cells (mainly macrophages and T lymphocytes), which was related to plaque vulnerability [56]. Several studies proved that the enhancement grade and enhancement ratio of culprit plaques were associated with the occurrence of stroke among patients with acute ischemic events [57, 58]. Irregular plaque surface was another vulnerable plaque feature that indicated fibrous cap rupture and was associated with symptomatic intracranial atherosclerosis [12, 59]. Our studies also demonstrated a higher risk of AIS in patients with irregular culprit plaque surface. These findings demonstrated that the structural characteristics of CoW are potential clinical predictors of AIS and TIA in patients with symptomatic ICAS. Xiao et al. found that higher NWI was associated with AIS [57]. Liang et al. demonstrated positive remodeling was closely correlated with ischemic stroke [58]. Another study focused on the culprit plaque features and hemodynamic changes in AIS and TIA populations [37]. However, their results showed

intraplaque hemorrhage and the Anterograde scores were associated with patients with stroke [37]. The reasons for these different results may be explained by different enrolled patients between ours and these above studies. All the above-mentioned studies only included patients with MCA events. In addition, Xiao et al. included more than half of the patients (49, 56.3%) with 30–69% symptomatic stenosis in the MCA [57]. Furthermore, intracranial atherosclerosis often involves multiple vessel beds. Wu et al. found an increased number of intracranial plaques was one of the independent risk factors for recurrent stroke [16]. In our study, we evaluated all the large intracranial vessels and measured all the plaque features downstream (bilateral MCA, ACA and PCA) of CoW. We found that irregularity of plaque surfaces, enhancement grade 2, and incomplete symptomatic side P-CoW were associated with AIS, which indicated that multiple plaques may relate to multiple stenoses in the large vessels. This would reduce cerebral blood flow and increase the risk of stroke.

Limitations

There are limitations to our study. Firstly, our study was a cross-sectional study, which needed to select a sample of subjects from a large and heterogeneous study population. Therefore, it could be susceptible to sampling bias and difficult to make a causal inference. Our study the univariable and multivariable regression analysis to control for confounding. However, other potential variables associated with the exposure and outcome might still be neglected. In our study, the clinical risk factors and the variables were chosen through works of literature and the clinical experiences of physicians. In the future, longitudinal follow-up study should be performed to evaluate the effect of the incomplete CoW on plaques and brain circulation. Secondly, our study speculated that the incomplete CoW resulted in the cerebral hemodynamic changes and induced vulnerability of the culprit plaques. However, we did not directly measure the hemodynamic changes in the brains of the study subjects and the effects of the vulnerability of the culprit plaques based on complete or incomplete CoW. Therefore, our results require further verification by computational fluid dynamics studies. Thirdly, the sample size in this study was small and may have resulted in biased results. Therefore, large sample studies are needed to confirm our results in the future.

Conclusions

This study demonstrated that incomplete CoW, both A-CoW and P-CoW, was significantly associated with differential atherosclerotic culprit plaque characteristics. Furthermore, incomplete symptomatic side P-CoW and

irregular plaque surface were independently associated with AIS.

Abbreviations

| | |
|----------------------|---------------------------------------------------------------------------------------------------------------------------|
| A-CoW | Anterior circle of Willis |
| AIS | Acute ischemic stroke |
| ARR | Arterial remodeling ratio |
| CER | Contrast enhancement ratio |
| CoW | Circle of Willis |
| DSA | Digital subtraction angiography |
| DSC-PWI | Dynamic susceptibility contrast-enhanced perfusion weighted imaging |
| DWI | Diffusion weighted imaging |
| HR-VWI | High-resolution vessel wall imaging |
| HT ₁ S | High T ₁ signals |
| ICAS | Intracranial atherosclerosis |
| IR-SPACE | Inversion-recovery prepared sampling perfection with application-optimized contrast using different flip angle evolutions |
| LA _{ref} | Reference lumen area |
| MCA | Middle cerebral artery |
| MPR | Multipolar reformation |
| MR | Magnetic resonance |
| MRA | Magnetic resonance angiography |
| NIHSS | National Institutes of Health Stroke Scale |
| NWA | Normalized wall area |
| NWI | Normalized wall index |
| P-CoW | Posterior circle of Willis |
| SI | Signal intensity |
| STAGE | Strategically acquired gradient echo |
| TIA | Transient ischemic attacks |
| TOF | Time of flight |
| WA _{lesion} | Wall area of the lesion |
| WSS | Wall shear stress |

Supplementary Information

The online version contains supplementary material available at <https://doi.org/10.1186/s12968-023-00931-2>.

Additional file 1. TableS1. Imaging parameters of all the MRI sequences. **Fig. S1.** One case presented with right eye blurred vision and right limb numbness and diagnosed with TIA 3 days before HR-VWI examination. **Fig. S2.** Representative multiplanar reformation (MPR) images for the vessel from the workstation. **Fig.S3.** Representative multiplanar reformation (MPR) images showed plaques and stenosis in a 70-year-old female with right lower limb weakness for 3 days. **Fig.S4.** Plaque and infundibulum signal intensity measurements. **Fig.S5.** Representative CMR images of a 47-year-old man with a history of hypertension, diabetes mellitus, and smoking who developed symptoms of paroxysmal right upper extremity weakness and was diagnosed with TIA 2 days before the CMR. **TableS2.** Inter-reader and intra-reader reliability of the plaque characteristics and anterograde scores [wh1] [wh1] [wh1] Response to R1-(14). **Fig. S6.** One case reported sudden slurring of speech for 2 days before HR-VWI examination. **Fig. S7.** One case reported right upper limb weakness for 4 days before HR-VWI examination.

Acknowledgements

We would like to express our gratitude to Professor E. Mark Haacke of Wayne State University, who helped us with English spelling and grammar, as well as with the structure of the manuscript. We thank all the neurologists and medical radiation technologists in our hospital.

Author contributions

HW and LS: substantial contributions to conception and design, acquisition of data, or analysis and interpretation of data; performing statistical analyses; drafting the article or revising it critically for important intellectual content; final approval of the version to be published. CZ and SL: contributions to conception and design; evaluation and acquisition of data; final approval of

the version to be published. GW, HW, and BW: contributions to conception and design; evaluation and acquisition of data; final approval of the version to be published. JZ and JD: analysis and interpretation of data; final approval of the version to be published. ZG: substantial contributions to conception and design; analysis and interpretation of data; revising it critically for important intellectual content; final approval of the version to be published. CC: substantial contributions to conception and design; drafting the article or revising it critically for important intellectual content; final approval of the version to be published; agreement to be accountable for all aspects of the work in ensuring that questions related to the accuracy or integrity of any part of the work are appropriately investigated and resolved. SX: substantial contributions to conception and design; drafting the article or revising it critically for important intellectual content; final approval of the version to be published; agreement to be accountable for all aspects of the work in ensuring that questions related to the accuracy or integrity of any part of the work are appropriately investigated and resolved. HW and LS contributed equally to this work. All authors read and approved the final manuscript.

Funding

This work was supported by the Natural Scientific Foundation of China (82171916 to S.X.; 81871342 to S.X.; 81901728 to C.C.); the Natural Scientific Foundation of Tianjin (21CYJC01580 to S.X.; 21JCQNJC01480 to C.C.); Tianjin Health Science and technology project (Specific projects of key disciplines) (TJWJ2022XK019); Tianjin Key Medical Discipline (Specialty) Construction Project (TJYXZDXK-041A).

Data availability

The datasets used and/or analysed during the current study are available from the corresponding author on reasonable request.

Declarations

Ethical approval and consent to participate

This retrospective study was approved by the Ethics committee of Tianjin First Central Hospital (2017N002KY). All subjects provided a written informed consent form.

Human and animal ethics

All the study participants were in accordance with the Declaration of Helsinki.

Consent for publication

All the authors finally approved of the version to be published.

Competing interests

The authors have no conflicts of interest to declare.

Author details

¹The School of Medicine, Nankai University, Tianjin 300071, China. ²Department of Radiology, First Central Clinical College, Tianjin Medical University, Tianjin 300192, China. ³Department of Radiology, Tianjin Huanhu Hospital, Tianjin 300350, China. ⁴Department of Radiology, Affiliated Hospital of Inner Mongolia Medical University, Hohhot 010000, China. ⁵MR Collaboration, Siemens Healthineers Ltd., Beijing 100102, China. ⁶Department of Neurology, School of Medicine, Tianjin First Central Hospital, Nankai University, Tianjin 300192, China. ⁷Department of Radiology, School of Medicine, Tianjin First Central Hospital, Nankai University, Tianjin 300192, China. ⁸Tianjin Institute of Imaging Medicine, Tianjin 300192, China.

Received: 29 May 2022 Accepted: 13 March 2023

Published online: 06 April 2023

References

- Banerjee C, Chimowitz MI. Stroke caused by atherosclerosis of the major intracranial arteries. *Circul Res*. 2017;120:502–13.
- Adnan I, Qureshi LRC. Intracranial atherosclerosis. *Lancet*. 2014;9921:984–98.
- Bang OY. Intracranial atherosclerosis: current understanding and perspectives. *J Stroke*. 2014;1:27–35.
- Hankey GJ. Stroke. *Lancet*. 2017;10069:641–54.
- Collaborators GN. Global, regional, and national burden of neurological disorders, 1990–2016: a systematic analysis for the global burden of Disease Study 2016. *Lancet Neurol*. 2019;5:459–80.
- Kasner SE, Chimowitz MI, Lynn MJ, et al. Predictors of ischemic stroke in the territory of a symptomatic intracranial arterial stenosis. *Circulation*. 2006;113:555–63.
- Marc I, Chimowitz MJLC. Stenting versus Aggressive Medical Therapy for Intracranial arterial stenosis. *N Engl J Med*. 2011;1:993–1003.
- Bos D, Portegies ML, van der Lugt A, et al. Intracranial carotid artery atherosclerosis and the risk of stroke in whites: the Rotterdam Study. *JAMA Neurol*. 2014;71:405–11.
- Dieleman N, van der Kolk AG, Zwanenburg JJ, et al. Imaging intracranial vessel wall pathology with magnetic resonance imaging: current prospects and future directions. *Circulation*. 2014;130:192–201.
- Swartz RH, Bhuta SS, Farb RI, et al. Intracranial arterial wall imaging using high-resolution 3-tesla contrast-enhanced MRI. *Neurology*. 2009;72:627–34.
- Gong Y, Cao C, Guo Y, et al. Quantification of intracranial arterial stenotic degree evaluated by high-resolution vessel wall imaging and time-of-flight MR angiography: reproducibility, and diagnostic agreement with DSA. *Eur Radiol*. 2021;31:5479–89.
- Zhang T, Tang R, Liu S, et al. Plaque characteristics of middle cerebral artery assessed using strategically acquired gradient echo (STAGE) and vessel wall MR contribute to misery downstream perfusion in patients with intracranial atherosclerosis. *Eur Radiol*. 2021;31:65–75.
- Song X, Zhao X, Liebeskind DS, et al. Associations between systemic blood pressure parameters and intraplate hemorrhage in symptomatic intracranial atherosclerosis: a high-resolution MRI-based study. *Hypertens Res*. 2020;43:688–95.
- Fakih R, Roa JA, Bathla G, et al. Detection and quantification of symptomatic atherosclerotic plaques with high-resolution imaging in Cryptogenic Stroke. *Stroke*. 2020;51:3623–31.
- Ran Y, Wang Y, Zhu M, et al. Higher plaque burden of middle cerebral artery is associated with recurrent ischemic stroke: a quantitative magnetic resonance imaging study. *Stroke*. 2020;51:659–62.
- Wu G, Wang H, Zhao C, et al. Large Culprit Plaque and more intracranial plaques are Associated with recurrent stroke: a case-control study using Vessel Wall Imaging. *Am J Neuroradiol*. 2022;43:207–15.
- Qiu C, Zhang Y, Xue C, Jiang S, Zhang W. MRA Study on Variation of the Circle of Willis in Healthy Chinese Male Adults. *Biomed Res Int*. 2015;2015:976340.
- Klimek-Piotrowska W, Rybicka M, Wojnarska A, Wojtowicz A, Koziej M, Holda MK. A multitude of variations in the configuration of the circle of Willis: an autopsy study. *Anat Sci Int*. 2016;91:325–33.
- Krabbe-Hartkamp MJ, van der Grond J, de Leeuw FE, et al. Circle of Willis: morphologic variation on three-dimensional time-of-flight MR angiograms. *Radiology*. 1998;207:103–11.
- Raluca Pascalau VAPD. The geometry of the Circle of Willis Anatomical Variants as a potential cerebrovascular risk factor. *Turk Neurosurg*. 2019;2:151–8.
- De Caro J, Ciacciarelli A, Tessitore A, et al. Variants of the circle of Willis in ischemic stroke patients. *J Neurol*. 2021;268:3799–807.
- Yu YN, Li ML, Xu YY, et al. Middle cerebral artery geometric features are associated with plaque distribution and stroke. *Neurology*. 2018;91:e1760–9.
- Kim BJ, Kim HY, Jho W, et al. Asymptomatic basilar artery plaque distribution and vascular geometry. *J Atheroscler Thromb*. 2019;26:1007–14.
- Lehoux S, Jones EA. Shear stress, arterial identity and atherosclerosis. *Thromb Haemost*. 2016;115:467–73.
- Li J, Zheng L, Yang WJ, Sze-To CY, Leung TW, Chen XY. Plaque wall distribution pattern of the atherosclerotic Middle Cerebral Artery Associates with the Circle of Willis completeness. *Front Neurol*. 2020;11:599459.
- Ginsberg MD. The cerebral collateral circulation: relevance to pathophysiology and treatment of stroke. *Neuropharmacology*. 2018;134:280–92.
- Easton JD, Saver JL, Albers GW, healthcare professionals from the American Heart Association/American Stroke Association Stroke Council. (2009) Definition and evaluation of transient ischemic attack: a scientific statement for ; Council on Cardiovascular Surgery and

- Anesthesia; Council on Cardiovascular Radiology and Intervention; Council on Cardiovascular Nursing; and the Interdisciplinary Council on Peripheral Vascular Disease. The American Academy of Neurology affirms the value of this statement as an educational tool for neurologists. *Stroke* 40:2276–2293
28. Tang R, Zhang Q, Chen Y, et al. Strategically acquired gradient echo (STAGE)-derived MR angiography might be a superior alternative method to time-of-flight MR angiography in visualization of leptomeningeal collaterals. *Eur Radiol*. 2020;30:5110–9.
 29. Mendelson SJ, Prabhakaran S. Diagnosis and management of transient ischemic attack and Acute ischemic stroke: a review. *JAMA*. 2021;325:1088–98.
 30. Zhou C, Yuan C, Li R, Wang W, Li C, Zhao X. Association between Incomplete circle of willis and carotid vulnerable atherosclerotic plaques. *Arterioscler Thromb Vasc Biol*. 2018;38:2744–9.
 31. Fan Z, Yang Q, Deng Z, et al. Whole-brain intracranial vessel wall imaging at 3 Tesla using cerebrospinal fluid-attenuated T1-weighted 3D turbo spin echo. *Magn Reson Med*. 2017;77:1142–50.
 32. Krol AL, Coutts SB, Simon JE, Hill MD, Sohn CH, Demchuk AM. Perfusion MRI abnormalities in speech or motor transient ischemic attack patients. *Stroke*. 2005;36:2487–9.
 33. Lindenholtz A, van der Kolk AG, van der Schaaf IC, et al. Intracranial atherosclerosis assessed with 7-T MRI: evaluation of patients with ischemic stroke or transient ischemic attack. *Radiology*. 2020;295:162–70.
 34. Lindenholtz A, van der Kolk AG, Zwanenburg J, Hendrikse J. The use and pitfalls of intracranial vessel wall imaging: how we do it. *Radiology*. 2018;286:12–28.
 35. Cao X, Yang Q, Tang Y, et al. Normalized wall index, intraplaque hemorrhage and ulceration of carotid plaques correlate with the severity of ischemic stroke. *Atherosclerosis*. 2020;315:138–44.
 36. Qiao Y, Anwar Z, Intrapromkul J, et al. Patterns and implications of intracranial arterial remodeling in Stroke Patients. *Stroke*. 2016;47:434–40.
 37. Liu S, Tang R, Xie W, et al. Plaque characteristics and hemodynamics contribute to neurological impairment in patients with ischemic stroke and transient ischemic attack. *Eur Radiol*. 2021;31:2062–72.
 38. Furuichi K, Ishikawa A, Uwabe C, Makishima H, Yamada S, Takakuwa T. Variations of the circle of willis at the end of the human embryonic period. *Anat Rec (Hoboken)*. 2018;301:1312–9.
 39. Nixon AM, Gunel M, Sumpio BE. The critical role of hemodynamics in the development of cerebral vascular disease. *J Neurosurg*. 2010;112:1240–53.
 40. Zarrinkoob L, Ambarki K, Wahlin A, Birgander R, Eklund A, Malm J. Blood flow distribution in cerebral arteries. *J Cereb Blood Flow Metab*. 2015;35:648–54.
 41. Alnaes MS, Isaksen J, Mardal KA, Romner B, Morgan MK, Ingebrigtsen T. Computation of hemodynamics in the circle of Willis. *Stroke*. 2007;38:2500–5.
 42. Groen HC, Gijzen FJ, van der Lugt A, et al. Plaque rupture in the carotid artery is localized at the high shear stress region: a case report. *Stroke*. 2007;38:2379–81.
 43. Tang D, Teng Z, Canton G, et al. Sites of rupture in human atherosclerotic carotid plaques are Associated with High Structural stresses an in vivo MRI-Based 3D fluid-structure Interaction Study. *Stroke*. 2009;40:3258–63.
 44. Samady H, Eshtehardi P, McDaniel MC, et al. Coronary artery wall shear stress is associated with progression and transformation of atherosclerotic plaque and arterial remodeling in patients with coronary artery disease. *Circulation*. 2011;124:779–88.
 45. Leng X, Lan L, Ip HL, et al. Hemodynamics and stroke risk in intracranial atherosclerotic disease. *Ann Neurol*. 2019;85:752–64.
 46. Millon A, Bousset L, Brevet M, et al. Clinical and histological significance of gadolinium enhancement in carotid atherosclerotic plaque. *Stroke*. 2012;43:3023–398.
 47. Derksen WJ, Peeters W, van Lammeren GW, et al. Different stages of intra-plaque hemorrhage are associated with different plaque phenotypes: a large histopathological study in 794 carotid and 276 femoral endarterectomy specimens. *Atherosclerosis*. 2011;218:369–77.
 48. Andreas Schindler RSNA. Prediction of stroke risk by detection of hemorrhage in carotid plaques: meta-analysis of individual patient data. *JACC Cardiovasc Imaging*. 2019;2:395–406.
 49. Shi Z, Li J, Zhao M, et al. Quantitative Histogram Analysis on Intracranial atherosclerotic plaques a high-resolution magnetic resonance imaging study. *Stroke*. 2020;51:2161–9.
 50. Zhang CDWJS. High-resolution Vessel Wall MR Imaging in diagnosis and length measurement of cerebral arterial thrombosis a feasibility study. *J Magn Reson Imaging*. 2022;56:1267–74.
 51. Henderson RD, Eliasziw M, Fox AJ, Rothwell PM, Barnett HJ. Angiographically defined collateral circulation and risk of stroke in patients with severe carotid artery stenosis. North american symptomatic carotid endarterectomy trial (NASCET) Group. *Stroke*. 2000;31:128–32.
 52. Chuang YM, Liu CY, Pan PJ, Lin CP. Posterior communicating artery hypoplasia as a risk factor for acute ischemic stroke in the absence of carotid artery occlusion. *J Clin Neurosci*. 2008;15:1376–81.
 53. Kim KM, Kang HS, Lee WJ, Cho YD, Kim JE, Han MH. Clinical significance of the circle of Willis in intracranial atherosclerotic stenosis. *J NeuroInterventional Surg*. 2016;8:251–5.
 54. Lin E, Kamel H, Gupta A, RoyChoudhury A, Girgis P, Glodzik L. Incomplete circle of Willis variants and stroke outcome. *Eur J Radiol*. 2022;153:110383.
 55. Chen JWWB. Vulnerable plaque imaging. *Neuroimaging Clin N Am*. 2005;3:609–21.
 56. Jeziorska M, Woolley DE. Local neovascularization and cellular composition within vulnerable regions of atherosclerotic plaques of human carotid arteries. *J Pathol*. 1999;188:189–96.
 57. Xiao J, Padrick MM, Jiang T, et al. Acute ischemic stroke versus transient ischemic attack: Differential plaque morphological features in symptomatic intracranial atherosclerotic lesions. *Atherosclerosis*. 2021;319:72–8.
 58. Liang J, Guo J, Liu D, Shi C, Luo L. Application of high-resolution CUBE sequence in exploring stroke mechanisms of atherosclerotic stenosis of Middle cerebral artery. *J Stroke Cerebrovasc Dis*. 2019;28:156–62.
 59. Song JW, Pavlou A, Xiao J, Kasner SE, Fan Z, Messé SR. Vessel Wall magnetic resonance imaging biomarkers of symptomatic intracranial atherosclerosis. *Stroke*. 2021;52:193–202.

Publisher's Note

Springer Nature remains neutral with regard to jurisdictional claims in published maps and institutional affiliations.

Ready to submit your research? Choose BMC and benefit from:

- fast, convenient online submission
- thorough peer review by experienced researchers in your field
- rapid publication on acceptance
- support for research data, including large and complex data types
- gold Open Access which fosters wider collaboration and increased citations
- maximum visibility for your research: over 100M website views per year

At BMC, research is always in progress.

Learn more biomedcentral.com/submissions

